

Windblown sand saltation: A statistical approach to fluid threshold shear velocity

*Original*

Windblown sand saltation: A statistical approach to fluid threshold shear velocity / Raffaele, L., Bruno, L., Pellerey, F., Preziosi, L.. - In: AEOLIAN RESEARCH. - ISSN 1875-9637. - 23:(2016), pp. 79-91. [10.1016/j.aeolia.2016.10.002]

*Availability:*

This version is available at: 11583/2662906 since: 2020-02-17T21:00:29Z

*Publisher:*

Elsevier

*Published*

DOI:10.1016/j.aeolia.2016.10.002

*Terms of use:*

This article is made available under terms and conditions as specified in the corresponding bibliographic description in the repository

*Publisher copyright*

(Article begins on next page)

# Windblown Sand Saltation: a statistical approach to threshold shear velocity

Lorenzo Raffaele<sup>a,d,\*</sup>, Luca Bruno<sup>b,d</sup>, Franco Pellerey<sup>c</sup>, Luigi Preziosi<sup>c,d</sup>

<sup>a</sup>Politecnico di Torino, Department of Structural, Geotechnical and Building Engineering,  
Corso Duca degli Abruzzi 24, I-10129, Torino, Italy

<sup>b</sup>Politecnico di Torino, Department of Architecture and Design,  
Viale Mattioli 39, I-10125, Torino, Italy

<sup>c</sup>Politecnico di Torino, Department of Mathematical Sciences,  
Corso Duca degli Abruzzi 24, I-10129, Torino, Italy

<sup>d</sup>Windblown Sand Modeling and Mitigation joint research group

---

## Abstract

The reliable prediction in probabilistic terms of the aeolian events magnitude is a key element for human activities in arid regions. Threshold shear velocity is in turn a key component of such a prediction. It suffers the effects of a number of uncertainties, such as the ones related to the physical phenomena, measurement procedures, and modelling. Semi empirical models are often fitted to a small amount of data, while recent probabilistic models needs the probability distribution of a number of random variables. Triggered by this motivation, this paper proposes a purely statistical approach to threshold shear velocity for sands, treated as a single comprehensive random variable. The data ensemble is defined collecting a huge number of studies available in literature. Estimates of probability density functions of threshold shear velocity for given sand classes are obtained. The obtained statistical moments are critically compared to some deterministic semi empirical models refitted to the same collected data. The proposed statistical approach allows to obtain high order statistics useful for practical purposes.

*Keywords:* windblown sand, saltation, threshold shear velocity, uncertainty, statistics

---

## 1. Introduction

Aeolian sand transport is a complex process that is induced by the interaction between subfields such as wind, air suspended particles and bed-particles. It contributes to soil erosion and landform evolution. Understanding and modeling its features is of fundamental interest in many research fields. Beside the importance of windblown sand and dust to the Earth sciences (Kok et al., 2012), from the engineering perspective, simulating windblown sand phenomena is relevant because of the interaction with a number of human activities and related infrastructures in arid environments (e.g. Middleton and Sternberg, 2013; Rizvi, 1989; Alghamdi and Al-Kahtani, 2005; Zhang et al., 2007; Cheng and Xue, 2014). In the infrastructure design perspective and within a probabilistic approach to design, the engineer is interested in relating a sand erosion or transport condition to a given, preferably low enough, probability of exceedance.

Among the transport mechanisms responsible of sand transport, saltation largely prevails in term of sand mass. The evaluation of the involved sand flux is usually given in term of sand transport rate by several laws, revised e.g. in Dong et al. (2003); Kok et al. (2012); Sherman and Li (2012). Most of such laws require the definition and evaluation of the fluid or static threshold, i.e. the value of the wind shear stress at which saltation is initiated. Usually, such a threshold is given in terms of fluid threshold shear velocity  $u_{st}$ . In turn, such a threshold value depends on a number

---

\*Corresponding author. Tel: (+39) 011.090.4870. Fax: (+39) 011.090.4999.

Email address: [lorenzo.raffaele@polito.it](mailto:lorenzo.raffaele@polito.it) (Lorenzo Raffaele)

URL: <http://www.polito.it/wsmm> (Lorenzo Raffaele)

16 of parameters belonging to both the wind and sand subfields.

17 Several authors have investigated such dependencies and proposed fluid threshold models, many of them reported e.g.  
18 in the overviews by [Shao \(2008\)](#); [Pye and Tsoar \(2009\)](#); [Merrison \(2012\)](#); [Kok et al. \(2012\)](#).

19 Systematic *experimental studies* addressed to  $u_{*t}$  versus the grain diameter  $d$  were carried out by e.g. [Bagnold \(1937\)](#),  
20 [Chepil \(1945\)](#), [Zingg \(1953\)](#), [Fletcher \(1976\)](#), [Iversen et al. \(1976\)](#). These measurements ground the consolidated  
21 literature data base. They are reported in Figure 1. A significant scatter among data can be observed notably at low  
22 values of the particle diameter. However, two general trend can be observed, divided by a local minimum at about  
23 75-100 $\mu\text{m}$  ([Kok et al., 2012](#)).

24 A number of *deterministic models* of the threshold shear velocity have been proposed in literature so far. They  
25 can be categorized in two classes with respect to both modelling scale and goal. *Microscopic models* discuss the  
26 equilibrium of the moments of the forces acting on the single particle resting on a bed of other particles ([Shao,  
27 2008](#)). They aim at pointing out the physical phenomena underlying each force and at modelling it. In a general  
28 framework, entraining aerodynamic forces (drag and lift ones) induce saltation, while stabilizing forces (gravitational  
29 and the interparticle ones) counteract them ([Greeley and Iversen, 1985](#); [Shao and Lu, 2000](#)). On one hand, the  
30 effective gravitational force including buoyancy, and the drag force correspond to well known phenomena and their  
31 modelling is widely accepted, see e.g. [Greeley and Iversen \(1985\)](#) and the cited reviews. On the other hand, the  
32 same does not hold for the other forces: the resultant lift force results from the Saffman one ([Saffman, 1965](#)) and  
33 the lift induced by vortical structures; the overall interparticle force results from several kinds of forces, including  
34 van der Waals forces, water adsorption forces and electrostatic forces. Although interparticle forces are expected to  
35 scale with the soil particle size (e.g. [Shao and Lu, 2000](#)), their modelling for aspherical and rough sand and dust  
36 remains poorly understood ([Kok et al., 2012](#)). In particular, such forces depend upon a number of parameters such  
37 as surface cleanliness, surface roughness at micro/nano meter scale, air and grain humidity, mineralogy and surface  
38 contaminants affecting hydrophilicity ([Merrison, 2012](#)). Semi-empirical *macroscopic models* aim at approximating  
39 the threshold shear velocity trend versus the particle diameter. Some of them are compared to the experimental data  
40 in Figure 1(a). Because of the above modelling difficulties, they do not analytically include the contribution of lift and  
41 interparticle forces while they explicitly retain the gravitational and drag ones. Any other contribution is accounted  
42 for in a semi empirical approach by introducing one or more free parameter(s), and the value of the latter obtained  
43 by fitting experimental data. The pioneering [Bagnold \(1941\)](#) model involves a single dimensionless constant  $A_B$ ,  
44 i.e. independent from the grain diameter or, in other terms, from Reynolds number: a monotonic increasing trend of  
45  $u_{*t}(d)$  results. The model by [Iversen and White \(1982\)](#) defines the same parameter  $A(\text{Re}_{*t})$  as a piece-wise empirical  
46 function of the friction Reynolds number  $\text{Re}_{*t}$  to mimic the effects of lift and interparticle forces: the resulting  $u_{*t}(d)$   
47 law is no longer monotonic and qualitatively reflect the trend of the experimental data. The model by [Shao and Lu  
48 \(2000\)](#) is more compact than the previous one. It neglects the  $\text{Re}_{*t}$  dependency, and at the same time generalizes the  
49 Bagnold one by introducing a novel correction term to account for the interparticle forces. A second dimensional  
50 constant free parameter  $\gamma$  [N/m] is included in the correction term. More recently, [McKenna \(2003\)](#) have considered  
51 the effect of soil moisture on the interparticle cohesive force by defining  $\gamma(\Delta P, d)$  as a function of the capillary-suction  
52 pressure deficit and of the grain diameter. Other laws of  $u_{*t}$  have been proposed for natural surfaces: they account  
53 for the effects of soil texture, soil moisture, salt concentration, surface crust, vegetation and/or pebbles on the surface.  
54 The review of such models is out of scope of the present paper: interested readers can refer to [Shao \(2008\)](#); [Webb and  
55 Strong \(2011\)](#).

56 The *probabilistic modelling approach* is a promising alternative to the deterministic one, having in mind that the  
57 modelling difficulties outlined above are mainly due to the uncertainties which affect the sand-acting forces ([Merrison,  
58 2012](#)). We suggest to ascribe such uncertainties to distinct comprehensive sources of uncertainty, that are:

- 59 • randomness of the *grain features*. Among these features, *grain size distribution* is traditionally recognized in  
60 literature as an important sand feature affecting  $u_{*t}$  (e.g. [Edwards and Namikas, 2015](#), and included references),  
61 beside the mean diameter. In fact, smaller particles interspersed among the large particles provide additional  
62 cohesive forces in natural sands, resulting in higher threshold conditions ([Roney and White, 2004](#)). The early  
63 studies on  $u_{*t}$  (e.g. [Bagnold, 1937](#)) usually assume nominally uniform sand, but this restriction clearly does not  
64 hold in a probabilistic framework. Others random/uncontrolled features are raised in literature, such as grain  
65 shape, surface microstructure (e.g. [Duan et al., 2013](#)), grain position relative to the other bed particles ([Phillips,  
66 1980](#)), grain mineralogy and surface cleanliness ([Merrison, 2012](#));

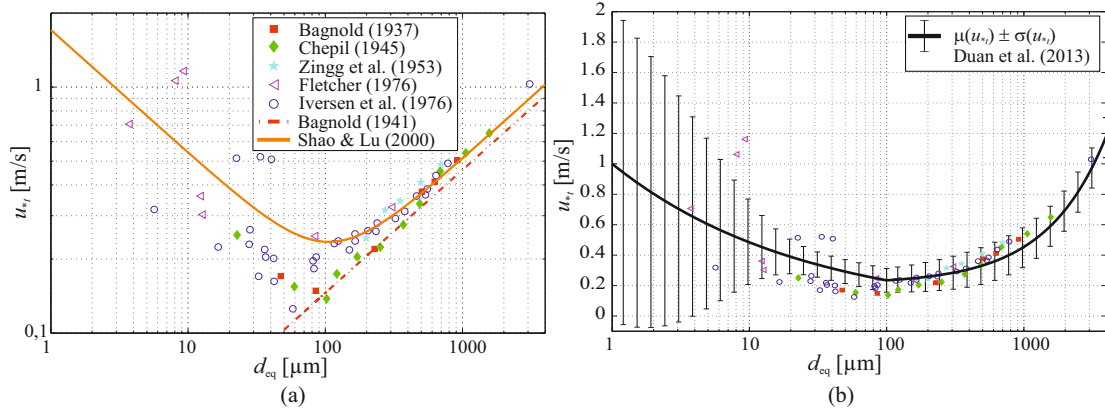


Figure 1: Threshold friction velocity: experimental data (symbols) compared with semi-empirical deterministic models (a, redrawn after Kok et al., 2012), and the probabilistic model by Duan et al. (2013) (b)

- the inborn variability of the *environmental conditions* even in wind tunnel facilities, e.g. air temperature and air relative humidity (e.g. Greeley and Iversen, 1985; Jones et al., 2002);
- *epistemic uncertainties* due to modelling, measurement procedures and techniques adopted to evaluate the bulk granulometry (Blott and Pye, 2006; Zhang et al., 2014) and/or the threshold shear velocity (Barchyn and Hugenholtz, 2011).

The smaller the grain size, the major the role of the interparticle forces, the higher the expected effect of the above uncertainties on the threshold shear velocity. Having this qualitative dependency in mind, Shao (2008) conjectured that while it is meaningful defining a threshold shear velocity as a single value for sand-sized particles, it is not meaningful to do the same for dust particles. This conjecture seems to be confirmed by the scatter of the experimental data at low values of  $d$  even for a common nominal setup condition (Figure 1a). Zimon (1982) first suggested to treat cohesive forces acting upon dust particles as random variables (r.v.s). He argued from experimental data that the cohesive forces probability distribution can be approximated by a lognormal one. Following Zimon's findings, Shao (2008) assumed that also the threshold shear velocity is log-normally distributed. Such an assumption looks questionable from an analytical point of view even by assuming the cohesive force the sole random variable among the grain acting forces: in fact,  $u_{*t}$  does not result from a simple rescaling of the cohesive force. Fueled by these problem features, Duan et al. (2013) have recently proposed a probabilistic model for threshold shear velocity. The study is grounded on a microscopic model, where the drag force, the electrostatic force, the gravity force and the cohesion force are described as functions of four microscopic r.v.s owing to the random nature of the microstructure of soil surface, of the particle shape and of positions in the bed irregular particle. The threshold shear velocity is then expressed as a function of these random quantities, some of them independent, some dependent, and its Probability Density Function (PDF) then evaluated through a statistical estimation of the distributions of the predictors. Subsequently, the mean value and standard deviation of the threshold shear velocity are fitted as functions of  $d$ . On one hand, the innovative model by Duan et al. (2013) has the merit to tackle for the first time the statistical characterization of the threshold shear velocity. On the other hand, the obtained results (Figure 1b) are not not entirely convincing. First, at very low values of  $d$ , mean value minus standard deviation  $\mu(u_{*t}) - \sigma(u_{*t})$  is negative, while  $u_{*t} \in \mathbb{R}^+$ . Second, the standard deviation  $\sigma(u_{*t})$  is monotonically increasing for  $d \geq 100$  μm and asymptotically tends to 0.132, while the scatter of experimental data clearly decreases for increasing  $d$ . Third, the mean  $\mu(u_{*t})$  is a linear function of  $d$  for  $d > 100$  μm, while its deterministic counterpart, i.e. the nominal values obtained by semi-empirical macroscopic models, is not. Finally, the study of Duan et al. (2013) does not evaluate high order statistical moments of the threshold shear velocity, i.e. skewness. In our opinion, such critical features can be ascribed to both modelling and technical difficulties. Among the former ones, the challenging task in writing a microscopic model inclusive of all the r.v.s affecting the sand grain acting forces. Among the second ones, the difficulties in obtaining probability

99 distribution for each microscopic r.v. from measurements and in handling mutually dependent r.v.s.

100 According to the authors, three main questions rise from the state of art briefly reviewed above: i. Is the determin-  
 101 istic approach able to face to the sources of uncertainties introduced above? ii. Is a statistical approach to the threshold  
 102 shear velocity required only for dust particles or for sand-sized particles too? iii. How to overcome the difficulties  
 103 encountered by probabilistic mechanical models in handling a number of microscopic r.v.s?

104 The present study aims at contributing in shedding some light on such issues. The deterministic approach is criti-  
 105 cally reconsidered in the light of a huge collection of experimental measurements. Then, a purely statistical approach  
 106 to threshold shear velocity is proposed, where the effects of all kinds of uncertainty sources are comprehensively  
 107 included and merged. Finally, the two approaches are compared.

108 The paper develops accordingly to the above objectives through the following sections. In Section 2 the collected  
 109 measurements and the resulting ensemble of selected data are described. In Section 3 some semi-empirical macro-  
 110 scopic models are refitted to the ensemble by means of non-linear regression. In Section 4 the statistical description of  
 111 the threshold shear velocity is given by referring to both analytical distributions (Subsect. 4.1) and the non-parametric  
 112 one (Subsect. 4.2). The deterministic and statistical approach are critically compared in Section 5, while conclusions  
 113 and research perspectives are outlined in Section 6.

## 114 2. Data collection and ensemble setting

115 The data already collected in Figure 1 are complemented by additional experimental measures collected from re-  
 116 view papers (Kok et al., 2012; Edwards and Namikas, 2015) and studies addressed to the evaluation of sand transport  
 117 rate for single particle diameters. Table 1 summarizes in chronological order the considered studies, while the com-  
 118 plete ensemble of retained sand experimental measurements of  $u_{*f}$  is plotted in Figure 2(a) versus  $d$ .

All studies test nominally dry granular matters. Except for Fletcher (1976) and Iversen et al. (1976), granular matter

Table 1: Collected setups: reference paper, number of samples, reference diameter

	#	$d$ [mm]
Bagnold (1937)	6	$0.05 \leq d \leq 0.92$
Chepil (1945)	11	$0.02 \leq d \leq 1.57$
Kawamura (1951)	2	0.25, 0.31
Zingg (1953)	5	$0.20 \leq d \leq 0.72$
Chepil (1959)	5	$0.20 \leq d \leq 0.72$
Belly (1964)	1	0.44
Kadib (1964)	1	0.15
Lyles and Krauss (1971)	3	$0.24 \leq d \leq 0.72$
Fletcher (1976)	7	$0.01 \leq d \leq 0.31$
Iversen et al. (1976)	33	$0.01 \leq d \leq 3.09$
Logie (1981)	4	$0.15 \leq d \leq 0.43$
Logie (1982)	1	0.24
Horikawa et al. (1983)	1	0.28
McKenna Neuman and Nickling (1989)	3	$0.19 \leq d \leq 0.51$
Nalpanis et al. (1993)	2	0.12, 0.19
Nicking and McKenna Neuman (1997)	1	0.20
Dong et al. (2002)	9	$0.13 \leq d \leq 0.90$
Dong et al. (2003)	9	$0.13 \leq d \leq 0.90$
Cornelis and Gabriels (2004)	3	$0.16 \leq d \leq 0.36$
McKenna Neuman (2004)	1	0.27
Roney and White (2004)	12	$0.31 \leq d \leq 0.39$

119 is sand and/or dust. For each considered study, the number # of the tested samples is given: an overall collection of  
 120

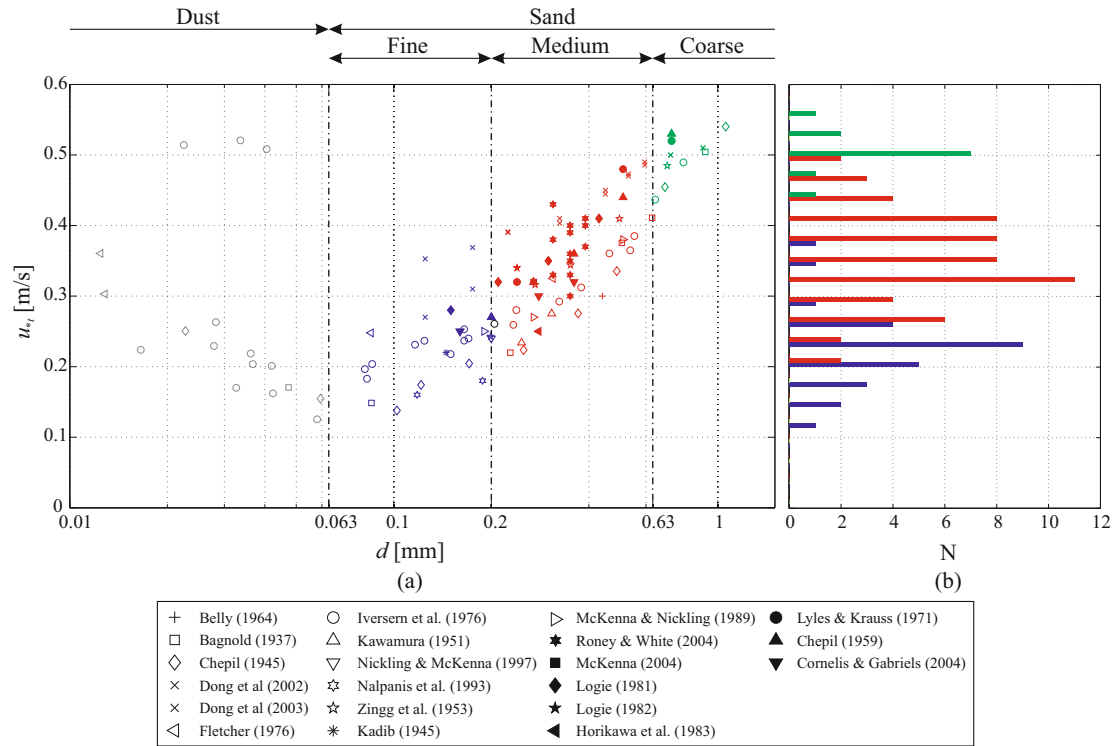


Figure 2: Threshold shear velocity measurements collected in literature (a), and their histograms for each sub-ensemble (b): fine (blue), medium (red), coarse (green) sands

121 120 setups follows. For each setup, the cited papers provide the grain mean, or median, diameter. In order to account  
 122 for the effect of different density of the grain constitutive materials, the equivalent particle diameter defined by [Chepil](#)  
 123 (1951); [Kok et al. \(2012\)](#) is evaluated. In Table 1 and in the following the equivalent reference diameter is noted as  $d$   
 124 for the sake of conciseness. In the rest of the paper,  $d$  is treated as a deterministic quantity.  
 125 A significant dispersion of the data can be easily observed in Figure 2(a), notably for fine and medium sands. In other  
 126 terms,  $u_{*t}$  takes different values at the same  $d$ . Such a feature suggests the ensembles are potentially constituted by  
 127 heterogeneous setups or, in other terms, setup parameters other than  $d$  are conjectured to affect the quantity of interest.  
 128 As anticipated in Sect. 1, several uncertain/uncontrolled parameters can be detailed for the considered studies.

- 129 • In the selected setups the *grain size distribution* is often qualitatively described, e.g. "as uniform as possible"  
 130 in [Bagnold \(1937\)](#), "very well and poorly sorted" in [Belly \(1964\)](#), "naturally graded" in [Kawamura \(1951\)](#).  
 131 Such a qualitative description is usually complemented by the nominal size-range of grains (e.g. [Bagnold,](#)  
 132 [1937](#); [Dong et al., 2003](#)), while in some papers the cumulative grain size distribution is plotted (e.g. [Belly,](#)  
 133 [1964](#); [Nalpanis et al., 1993](#); [Kawamura, 1951](#); [Nickling and McKenna Neuman, 1997](#); [Roney and White, 2004](#)).  
 134 Recently, [Edwards and Namikas \(2015\)](#) have made an effort to evaluate a measure of the diameter variability  
 135 by evaluating the sorting coefficient for a number of studies: in spite of some difficulties in obtaining such  
 136 a measure from nominal size-range, it is worth recalling that non negligible variability (e.g. sorting  $\approx 0.05$ ,  
 137 coefficient of variation  $c.o.v. \approx 0.12$  in [Chepil \(1959\)](#)) results also from sieving addressed to obtain sands as  
 138 uniform as possible. Even greater variability characterizes natural sands (e.g. sorting  $\approx 0.65$ ,  $c.o.v. \approx 0.35$  in  
 139 [Kawamura \(1951\)](#)). Other randomness of the grain features (e.g. grain shape, surface microstructure, grain  
 140 position relative to the other bed particles, grain mineralogy) are not specified in the collected studies.
- 141 • *Air humidity* during wind tunnel tests is given and systematically addressed only by [Kadib \(1964\)](#) to our best  
 142 knowledge.

- Analogously,  $u_{*t}$  measurements and post processing techniques are heterogeneous among the studies (Blott and Pye, 2006; Zhang et al., 2014), Roney and White (2004) prove their effects on fluid threshold shear velocity by adopting three different techniques.
- The quantitative definition of the fluid threshold shear velocity is not commonly adopted in all the studies, only Lyles and Krauss (1971) provide several  $u_{*t}$  values from visual observations depending on the kind of grain motion.

In short, the experimental data ensemble is naturally and inevitably affected by a huge number of uncertainties, belonging to both physical setup and epistemic uncertainty.

The present paper is devoted to the characterization of threshold shear velocity of sand only. Hence, setups adopting dust, i.e. having  $d < 0.063$  mm according to ISO14688-1:2002, are first discarded (empty light grey markers in Figure 2-a). An overall sand ensemble having  $\# = 97$  results. A deterministic dependency on  $d$  is clearly confirmed along the ensemble. Hence, on one hand, the definition of sub-ensemble is therefore advisable. On the other hand, the limited number of realization in the ensemble does not allow to define a huge number of sub-ensembles. Having these issues in mind, we gather realizations in three sand classes according to the common practice in aeolian geomorphology and referring to ISO14688-1:2002:

- Fine sand ( $0.063 < d \leq 0.2$  mm),  $\# = 27$ ;
- Medium sand ( $0.2 < d \leq 0.63$  mm),  $\# = 58$ ;
- Coarse sand ( $0.63 < d \leq 1.2$  mm),  $\# = 12$ .

It is worth noting that "very coarse" sand as defined by Friedman and Sanders (1978) is not included in the coarse sub-ensemble because scarceness of available experimental data. The histograms for each sub-ensemble are plotted in Figure 2(b). The adequateness of each sub-ensemble cardinality in providing accurate statistics will be carefully checked in the study.

### 3. Deterministic approach: non-linear regression

Prior to the statistical analysis of the sub-ensembles above, non-linear regression is applied to the whole collected data in order to refit some of the semi-empirical macroscopic models available in literature. The refitting objective is twofold: on the one hand, the field of application is limited to sands, i.e. on an entrainment physics simpler than the one governing dusts; on the other hand, model parameters are fitted to a number of data higher than the one originally adopted by the authors of the models. Bagnold (1941) (Eq.1) and Shao and Lu (2000) (Eq.2) models are selected because of their compactness, i.e. their dependence from a small number of empirical parameters ( $A_b$ ,  $A_s$  and  $\gamma$ ). The two semi-empirical models are

$$u_{*t} = A_b \sqrt{\frac{\rho_p - \rho_a}{\rho_a} g d}, \quad (1)$$

$$u_{*t} = A_s \sqrt{\frac{\rho_p - \rho_a}{\rho_a} g d + \frac{\gamma}{\rho_a d}}. \quad (2)$$

where  $\rho_p$  and  $\rho_a$  are particle and air density, respectively, and  $g$  is gravitational acceleration. Beside the single-valued estimates of a goodness of fit, for each model the prediction Confidence Intervals (CIs) are evaluated at 5<sup>th</sup> and 95<sup>th</sup> percentiles, i.e. the interval within which the true value is expected to lie. Figure 3 compares the refitted laws to the original ones, while the corresponding model parameters are summarized in Table 2. The following remarks can be outlined:

- generally speaking, the refitted laws predict higher values of  $u_{*t}$  for given  $d$ . It is worth pointing out that the ensemble includes a number of poorly sorted and natural sands, while the ensemble originally adopted by Bagnold (1941) and Shao and Lu (2000) were limited to sand as uniform as possible. Hence, interspersed small particles provide additional cohesive forces also for medium and coarse natural sands (Roney and White, 2004);

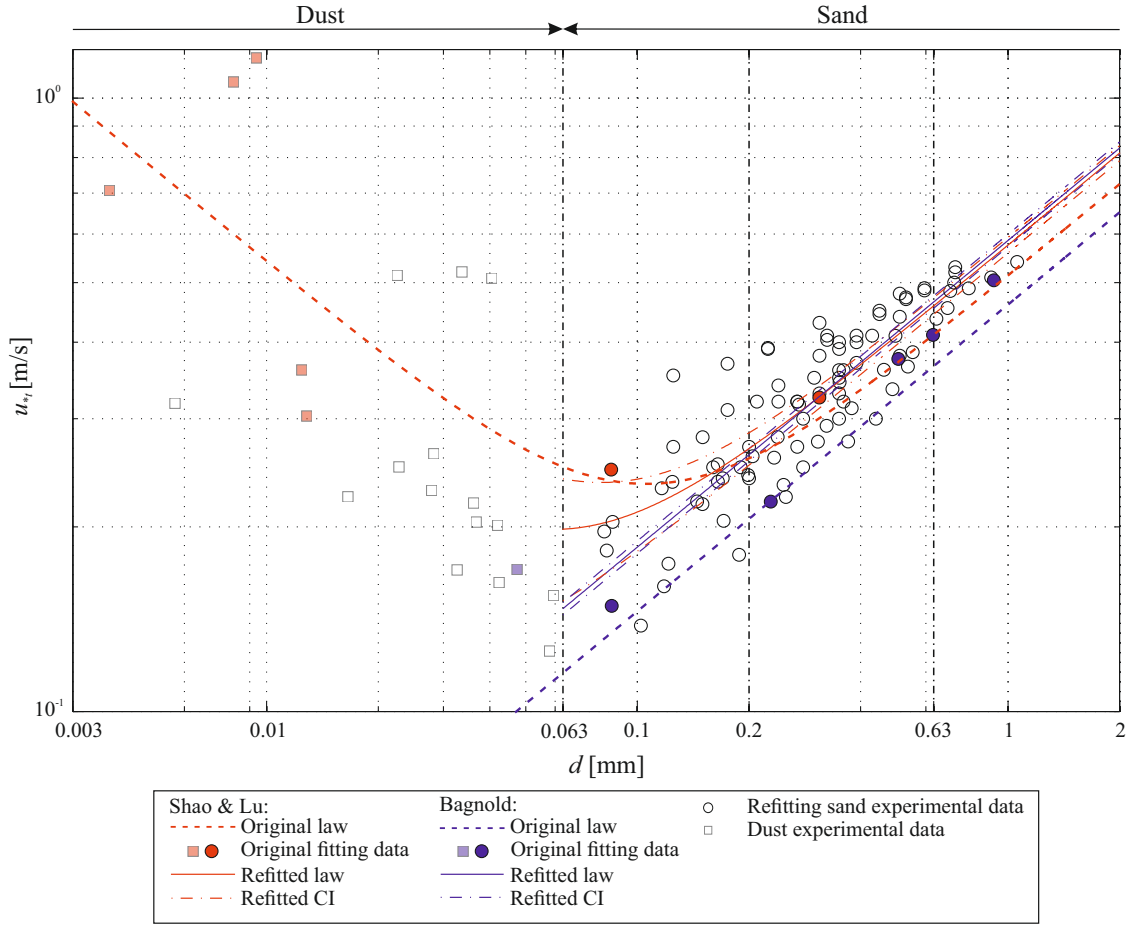


Figure 3: Non-linear regression and CIs for [Bagnold \(1941\)](#) and [Shao and Lu \(2000\)](#)

Table 2: Original and refitted model parameters

	Original parameters		Refitted parameters	
	<a href="#">Bagnold (1941)</a>	<a href="#">Shao and Lu (2000)</a>	<a href="#">Bagnold (1941)</a>	<a href="#">Shao and Lu (2000)</a>
$A$ [-]	0.100	0.111	0.127	0.125
$\gamma$ [N/m]	-	$2.9 \times 10^{-4}$	-	$9.15 \times 10^{-5}$
$R^2$	-	-	0.76	0.77

- 183 • both laws pretty agree for medium and coarse sands ( $d > 0.2$  mm), i.e. they share both the asymptotic trend  
184 due to the common dependency of  $u_{*t}$  on  $\sqrt{d}$ , and the intercept, i.e.  $A_b = 0.127 \approx A_s = 0.125$ . This finding  
185 is consistent with the spirit of the Shao's model, whose corrective term  $\gamma/\rho_a d$  is conceived to modify Banold's  
186 model at low  $d$  only;
- 187 • as regards [Shao and Lu \(2000\)](#) model, the refitted law predicts lower  $u_{*t}$  values for small  $d$  than the original one,  
188 because fitting is restricted to sands and exclude dusts. In other words, the refitted Shao's law mimics herein  
189 only the sand physics, and its trend at low  $d$  is not driven by the dust physics, and notably by the very high  
190 values  $u_{*t} \approx 0.5$  m/s provided by [Iversen et al. \(1976\)](#) at  $d = 0.023, 0.034, 0.041$  mm and  $u_{*t} > 1$  m/s provided

191 by Fletcher (1976) at  $d = 0.008, 0.009$  mm. A lower value of  $\gamma$  for the refitted law follows;

- 192 • CI of the Bagnold fitting is quite narrow (being the model easily reducible to a linear regression model). On  
193 the contrary, CI for Shao's model becomes wider as  $d$  decreases, because of the statistical uncertainty on the  
194 parameter  $\gamma$  in the term  $\gamma/(\rho_a d)$ , which has its main effects for small values of  $d$ ;
- 195 • for both fittings  $R^2 \approx 0.76$ . This value, although satisfying, highlights a shortcoming of the deterministic  
196 approach: both laws cross over different kind of sands (fine, medium, coarse), while distinct regimes can be  
197 expected in each sand class, notably as regards data dispersion and skewness.

## 198 4. Statistical approach

199 In the following a statistical approach is proposed, having in mind the shortcomings of the deterministic approach,  
200 and the perspective practical needs in design infrastructures in arid environments. In fact, engineers are interested in  
201 evaluating low percentiles of  $u_{*t}$ , i.e. values having not-exceedance low probability, which reflect in high percentiles  
202 of the transport rate, i.e. values having an exceedance low probability.

203 Within such an approach, each source of uncertainty and related microscopic parent r.v.s are not described in  
204 statistical terms, because of the lack of data. Conversely, the threshold shear velocity is adopted as a single compre-  
205 hensive r.v. On the one hand, its variability comprehensively includes and reflects the effects of all the parent r.v.s. On  
206 the other hand, the effects of a given single parent r.v. cannot be isolated.

207 The statistics of  $u_{*t}$  are obtained for each sub-ensemble resulting from the sand grading as illustrated in Sect. 2.

### 208 4.1. Analytical distributions fitting

209 Since the probability distributions of  $u_{*t}$  for the three size ranges are a priori unknown, we first aim at assessing if  
210 a parametric distribution can be adopted to describe the threshold shear velocity for each kind of sand. The data in  
211 each sub-ensemble are fitted to some guess reference distributions by means of the maximum likelihood estimation  
212 method. The considered distributions are normal, lognormal, and Weibull. Figure 4(a), (b), (c) collects the empirical  
213 and fitted Cumulative Distribution Functions (CDF). In order to assess the goodness of the fit, two approaches are  
214 used.

215 First, we employ the Anderson and Darling (1952) empirical distribution test because of the high weight placed  
216 on observations in the tails of distribution. The null hypothesis is never rejected, being the resulting  $p$ -values always  
217 greater than 0.1 for all tested distributions (with a range from 0.11 to 0.43 for fine sand, always greater than 0.5  
218 for medium sand, and with range a from 0.22 to 0.89 for coarse sand). In particular, for medium sand, the normal  
219 distribution obtains the largest  $p$ -value ( $p \approx 0.88$ ), while for coarse sand, the Weibull distribution is highly scored  
220 ( $p \approx 0.89$ ).

221 However, having in mind the high levels of probability of errors of the second kind in goodness of fit tests like  
222 Anderson and Darling (1952) dealing with small samples, and the fact that we are interested in evaluating extreme  
223 percentiles of  $u_{*t}$  (notably, the low ones), a second analysis based on the so-called quantile  $q-q$  plots is adopted as an  
224 exploratory visual aid to assess the local goodness of fitting of the reference distributions (Figure 4-d, e, f). The  $q-q$   
225 plots exam reveals that parametric distributions generally fail in describing experimental data. Only the goodness of  
226 normal fit is confirmed for medium sand ( $\mu(u_{*t}) = 0.355$  mm,  $\sigma(u_{*t}) = 0.068$  mm) also close to the tails, while a  
227 significant departure of the Weibull quantiles from bisector is observed at the lower tail for coarse sand.

### 228 4.2. Non-parametric distribution fitting

229 Since most of the parametric distributions do not seem able to correctly fit data in the tails, we decide to adopt a  
230 non-parametric density estimation based on kernel methods.

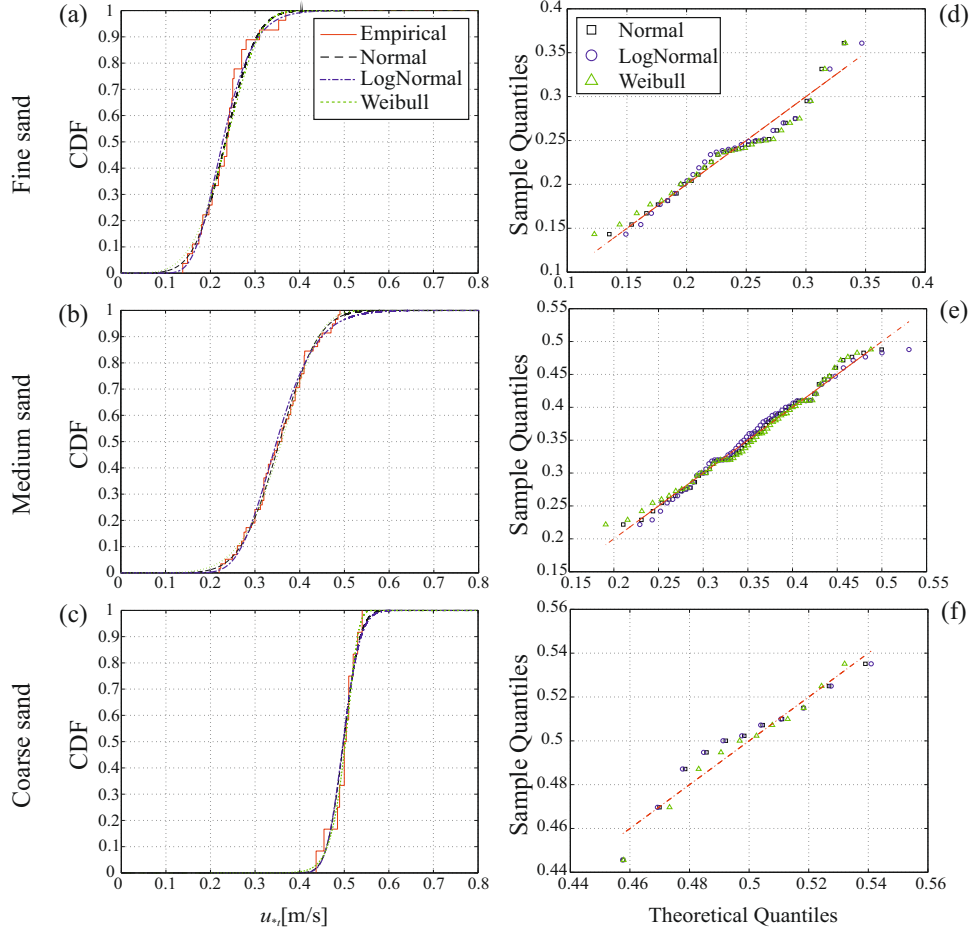


Figure 4: Analytical distribution results: cumulative distribution functions (a), (b), (c), and  $q-q$  plots (d), (e), (f) for fine, medium and coarse sand

#### 231 4.2.1. Adopted methods

The PDF kernel estimate method is based on representation of the density as a weighted sum of the kind

$$\hat{f}_h(x) = \sum_{i=1}^n K\left(\frac{x - x_i}{h}\right),$$

232 where the  $x_i$ 's are the observed values, the kernel  $K$  is a suitable unimodal probability density symmetric about zero,  
 233 while  $h$  is a suitable smoothing parameter known as the bandwidth of the estimate. While the choice of the kernel  $K$   
 234 seems not to affect too much a proper non-parametric estimate  $\hat{f}$  of the density  $f$  (commonly, Gaussian kernels are  
 235 applied), the specific choice of the bandwidth  $h$  controlling the smoothness of the resulting density curve is extremely  
 236 important, since the bias and the variance of the estimator  $\hat{f}$  strongly depend on  $h$  in a non-linear relation. In fact, the  
 237 Mean Integrated Square Error ( $MISE$ , Eq. 3)

$$MISE(h) = E \int (\hat{f}_h(x) - f(x))^2 dx, \quad (3)$$

238  
 239 which provides a measure of the difference between the estimate density function and the true density, can be expressed  
 240 as

$$MISE(h) = \int Bias^2(\hat{f}_h(y)) dy + \int Var(\hat{f}_h(y)) dy, \quad (4)$$

241 where  $Bias(\hat{f}_h(y)) = c_1 h^2 + o(h^2)$  and  $Var(\hat{f}_h(y)) = \frac{c_2}{h} + o(\frac{1}{h})$ , being  $c_1$  and  $c_2$  values depending on  $K$  and on the true  
 242 density  $f$  (see Sheather, 2004, for details).

243 Since the  $MISE$  is not mathematically tractable, common methods for bandwidth selection employ the Asymptotic  
 244 Mean Integrated Square Error ( $AMISE$ ), whose minimum as a function of  $h$  can be less hardly evaluated, as well as a  
 245 variety of alternative automatic, data-based methods. Among all, the most common are Plug-In (PI) and Least Squares  
 246 Cross-Validation (LSCV) bandwidth estimate methods. Both these two techniques provide good performances, but  
 247 while LSCV often shows tendency to undersmooth, PI tends to oversmooth in the case of densities with high fluctua-  
 248 tions (see, again Sheather, 2004), as our raw data suggest. Because of this reason, and since oversmoothing provides a  
 249 prudential approach in estimation of extreme quantiles (i.e., tends to estimate larger interquantiles differences), the PI  
 250 method is adopted. The Matlab ©Kernel Smoothing Toolbox developed by Koláček and Zelinka (2012) (see Horová  
 251 et al., 2012, for details) is used to numerically evaluate the values of  $h$  through the PI method and Gaussian kernels.

#### 252 4.2.2. Results

253 As anticipated, the convergence of the first two statistical moments is checked for increasing ensemble cardinality  
 254  $\# = n$ , i.e. number of data included in each sub-ensemble. The weighted residual of the generic parameter  $\varphi$   
 255 for growing cardinality of a sub-ensemble is defined as  $\varphi_{res,n} = |(\varphi_n - \varphi_{n-1})/\varphi_n|$ , and averaged over 20.000 random  
 permutations of the order of the data. Residual convergence versus  $n$  is plotted on loglog scale in Figure 5. The rate

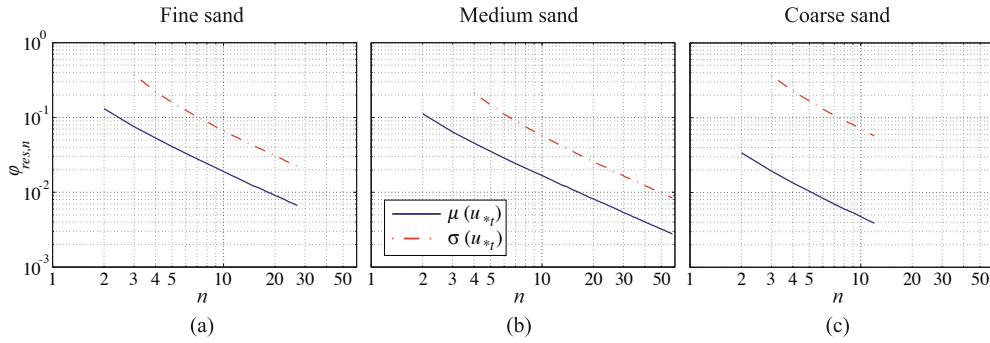


Figure 5: Convergence of the the mean  $\mu(u_{*t})$  and standard deviation  $\sigma(u_{*t})$  for each sub-ensemble (fine, medium and coarse sand)

256 of convergence is the same for both moments and for every sand class. Hence, the key element in convergence is  
 257 the cardinality of each sub-ensemble. The complete set of collected events allows one to reach a threshold of about  
 258  $3 \times 10^{-3} \leq \mu_{res,\#} \leq 7 \times 10^{-3}$  for the mean values, and of  $8 \times 10^{-3} \leq \sigma_{res,\#} \leq 6 \times 10^{-2}$  for the standard deviation. The  
 259 obtained final residual error is acceptable from a practical engineering point of view, except for the one of the standard  
 260 deviation for coarse sand (Figure 5-c). In spite of such an encouraging convergence, the fitting of high order moments  
 261 and extreme percentiles would benefit of higher cardinality of the sub-ensembles. We encourage further independent  
 262 experimental measurements to enrich the ensembles.

263 The non-parametric PDFs estimated from the complete sub-ensembles are shown in Figure 6(a), (b), (c), for fine,  
 264 medium and coarse sands, respectively. Statistical moments, such as mean values, standard deviations and skewness  
 265  $sk$ , coefficient of variation ( $c.o.v.$ ),  $1^{st}$  and  $3^{rd}$  quartiles, and  $5^{th}$  and  $95^{th}$  percentiles are obtained from the fitted  
 266 PDFs. They are summarized in Table 3. Remarkably, the non parametric estimate gives results coherent with the  
 267 goodness of fit assessment for the analytical distributions:  $u_{*t}$  for medium sand is confirmed to be pretty normally  
 268 distributed (Figure 6-b), with analogous mean value and standard deviation, and with a very low value of skewness  
 269 ( $sk = 0.033$ ). Conversely, the PDFs for fine and coarse sands are confirmed to be far from gaussian, positively and  
 270 negatively skewed, respectively. It is worth pointing out that, even if no constraints are a priori imposed on the support  
 271 of the non parametric PDFs, also the low percentiles are positive, i.e.  $p_5(u_{*t}) > 0$  for fine sand too. The monotonic  
 272 growth of both  $c.o.v.$  and skewness for decreasing reference diameter  $d$  properly reflects the expected growing role  
 273 played by interparticle forces and related uncertainties. In particular, the coefficient of variation for fine and medium  
 274 sands is about  $c.o.v. \approx 0.25$ : even if this is a relatively moderate  $c.o.v.$  value with respect to other environmental r.v.s  
 275 (e.g. turbulent wind velocity), it implies the  $5^{th}$  percentile is about 0.6 times the mean value.  
 276

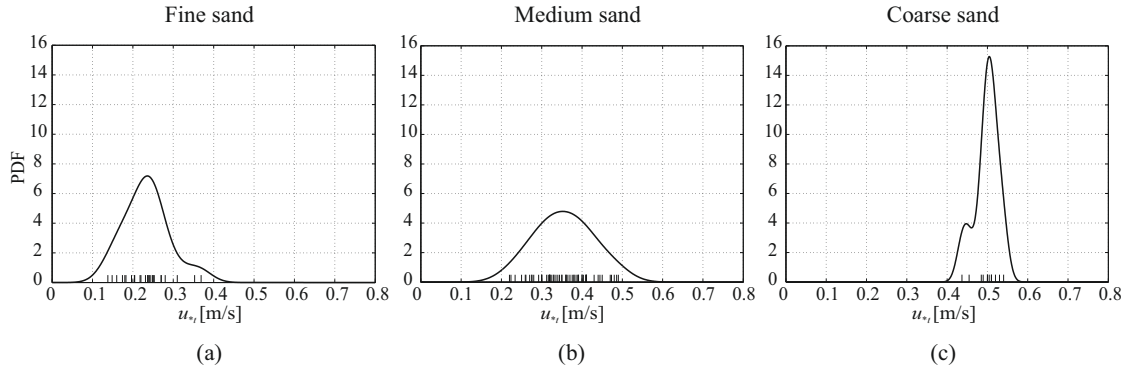


Figure 6: Non-parametric PDFs of the threshold shear velocity for fine, medium and coarse sands. Lower vertical bars stand for sand sample measurements

Table 3: Statistics of threshold shear velocity from non-parametric distributions

		Fine sand	Medium sand	Coarse sand
$\mu(u_{*t})$	[m/s]	0.234	0.355	0.498
$\sigma(u_{*t})$	[m/s]	0.062	0.080	0.032
$sk(u_{*t})$	[-]	0.360	0.033	-0.539
<i>c.o.v.</i>	[-]	0.266	0.224	0.063
$p_5(u_{*t})$	[m/s]	0.136	0.225	0.437
$Q_1(u_{*t})$	[m/s]	0.192	0.299	0.482
$Q_3(u_{*t})$	[m/s]	0.269	0.411	0.520
$p_{95}(u_{*t})$	[m/s]	0.351	0.488	0.544

## 277 5. Comparison between deterministic and statistical approach

278 Finally, the main findings of the proposed statistical approach are critically compared to the results of the deter-  
 279 ministic approach. In Figure 7(a) the mean values  $\mu(u_{*t})$  obtained from the non-parametric distribution for the three sand classes are superimposed to the refitted deterministic semi-empirical expressions of the nominal value of  $u_{*t}$ . It is

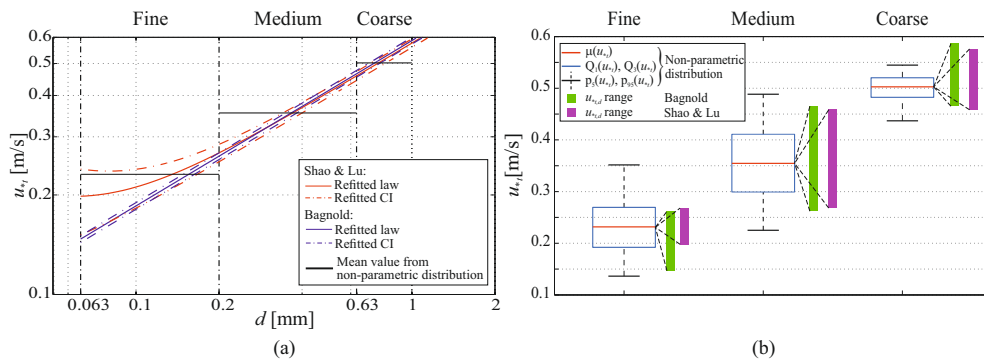


Figure 7: Comparison between statistical non-parametric distributions and semi-empirical deterministic models: mean values  $\mu(u_{*t})$  versus refitted Bagnold (1941) and Shao and Lu (2000) models (a), boxplots versus deterministic ranges (b)

281 clear that statistics over data for a given sand class, i.e. a given  $d$  range, implies the mean value has a step-wise trend  
282 versus the reference diameter  $d$ . In other words, the statistical approach apparently involves losing information with  
283 respect to the continuous deterministic laws  $u_{*t}(d)$ , if reference is made to the mean value only. In fact, this apparent  
284 under-sampling, is largely compensated by high-order statistics, that substantially enrich the description of  $u_{*t}$  for  
285 each sand class. In order to testify this feature, the box plots corresponding to the sand classes are plotted in Figure  
286 7(b) together with the corresponding deterministic range of the nominal values of the threshold shear velocity  $u_{*t,d}$   
287 predicted through Bagnold (1941) and Shao and Lu (2000) refitted models. From both Figures the role of skewness  
288 is clearly depicted: the mean value of  $u_{*t}$  as a r.v. is very close to the nominal value deterministically evaluated at the  
289 mid-range diameter  $d_m$  only for null skewness (medium sand); otherwise,  $\mu(u_{*t}) \geq u_{*t}(d_m)$  for  $sk > 0$  (fine sand) and  
290 viceversa (coarse sand). Finally, the statistical approach allows to associate a given probability of exceedance to any  
291 value of the threshold shear velocity, while the nominal value from a deterministic law does not.

## 292 6. Conclusions

293 The present study critically compares deterministic and statistical approaches to threshold shear velocity on the  
294 basis of the collection of a huge amount of experimental measurements collected ad hoc from literature. Since the de-  
295 scription of each random variable affecting  $u_{*t}$  is hard to be practically tractable, each source of uncertainty is merged  
296 within the single and comprehensive random variable  $u_{*t}$ .

297 Deterministic approach is updated thanks to the amount of collected data: in spite of a satisfying fitting of the  
298  $u_{*t}(d)$  nominal law, the lack of information about  $u_{*t}$  variability remains a shortcoming of the approach.

299 The proposed statistical approach allows to enrich the threshold shear velocity description providing measures  
300 of its variance and high order statistics, notably extreme percentiles. From a practical perspective in a number of  
301 application fields, the proper definition of  $u_{*t}$  values associated to given non exceedance probabilities allows to pre-  
302 dict aeolian events and in turn to assess the performances of mitigation measures in probabilistic terms. Moreover,  
303 statistics are obtained over broad sub-ensembles defined w.r.t. sand classes, rather than on narrow  $d$  intervals. From a  
304 practical perspective, this allows to apply the statistical approach to mesoscale problems (e.g. infrastructures crossing  
305 several landforms along their path), where a single local reference sand diameter (e.g. at a dune toe or crest) is no  
306 longer relevant.

307 In the light of the obtained results, we suggest two research perspectives. First, a high cardinality of the dataset  
308 allows the full convergence of the statistical estimates: hence, the authors hope that further independent experimental  
309 studies will enrich the data ensemble. Second, the uncertainty propagation from the threshold shear velocity to the  
310 sand transport rate would worth to be further investigated.

## 312 Acknowledgments

313 The study has been developed in the framework of the Windblown Sand Modeling and Mitigation joint research,  
314 development and consulting group established between Politecnico di Torino and Optiflow Company. The authors  
315 wish to thank Davide Fransos, member of the WSMM group, for the helpful discussions about the topics of the paper.  
316 The research that lead to the present paper was partially supported by a grant of the group GNFM of INdAM.

## 317 References

- 318 Alghamdi, A.A., Al-Kahtani, N.S., 2005. Sand Control Measures and Sand Drift Fences. *J. Perform. Constr. Facil.* 19, 295–299. doi:10.1061/  
319 (ASCE)0887-3828(2005)19:4(295).
- 320 Anderson, T., Darling, D., 1952. Asymptotic theory of certain goodness of fit criteria based on stochastic processes. *Ann. Math. Stat.* 23, 193–212.
- 321 Bagnold, R., 1941. *The Physics of Blown Sand and Desert Dunes*. Methuen. doi:10.1007/978-94-009-5682-7.
- 322 Bagnold, R.A., 1937. The transport of sand by wind. *Geogr. J.* 89, 409–38. doi:10.2307/1786411.
- 323 Barchyn, T.E., Hugenholtz, C.H., 2011. Comparison of four methods to calculate aeolian sediment transport threshold from field data: Implications  
324 for transport prediction and discussion of method evolution. *Geomorphology* 129, 190–203. doi:10.1016/j.geomorph.2011.01.022.
- 325 Belly, P.Y., 1964. Sand movement by wind. Technical Report 1. U.S. Army - Corps of Engineers. US Army Coastal Eng. Res. Center, Washington,  
326 DC.
- 327 Blott, S., Pye, K., 2006. Particle size distribution analysis of sand-sized particles by laser diffraction: an experimental investigation of instrument  
328 sensitivity and the effects of particle shape. *Sedimentology* 53, 671–685. doi:10.1111/j.1365-3091.2006.00786.x.

329 Cheng, J., Xue, C., 2014. The sand-damageprevention engineering system for the railway in the desert region of the qinghai-tibet plateau. *J. Wind*  
330 *Eng. Ind. Aerodyn.* 125, 30–37. doi:10.1016/j.jweia.2013.11.016.

331 Chepil, W., 1945. Dynamics of wind erosion: II. initiation of soil movement. *Soil Sci.* 60, 397–411. doi:10.1097/00010694-194511000-00005.

332 Chepil, W., 1959. Equilibrium of soil grains at threshold of movement by wind. *Soil Sci. Soc. Proc.* 23, 422–428.

333 Chepil, W.S., 1951. Properties of soil which influence wind erosion: IV. state of dry aggregate structure. *Soil Sci.* 72, 387–401.

334 Cornelis, W., Gabriels, D., 2004. A simple model for the prediction of the deflation threshold shear velocity of dry loose particles. *Sedimentology*  
335 51, 39–51.

336 Dong, Z., Liu, X., Wang, H., Wang, X., 2003. Aeolian sand transport: a wind tunnel model. *Sediment. Geol.* 161, 71–83. doi:10.1016/  
337 *S0037-0738(02)00396-2*.

338 Dong, Z., Liu, X., Wang, H., Zhao, A., Wang, X., 2002. The flux profile of a blowing sand cloud: a wind tunnel investigation. *Geomorphology* 49,  
339 219–230. doi:10.1016/S0169-555X(02)00170-8.

340 Duan, S.Z., Cheng, N., Xie, L., 2013. A new statistical model for threshold friction velocity of sand particle motion. *Catena* 104, 32–38.  
341 doi:10.1016/j.catena.2012.04.009.

342 Edwards, B., Namikas, S., 2015. Characterizing the sediment bed in terms of resistance to motion: Toward an improved model of saltation  
343 thresholds for aeolian transport. *Aeolian Res.* 19, 123–128. doi:10.1016/j.aeolia.2015.10.004.

344 Fletcher, B., 1976. Incipient motion of granular materials. *J. Phys. D Appl. Phys.* 9, 2471–8. doi:10.1088/0022-3727/9/17/007.

345 Friedman, G., Sanders, F., 1978. *Principles of sedimentology*. Wiley, New York.

346 Greeley, R., Iversen, J.D., 1985. *Wind as a Geological Process on Earth, Mars, Venus, and Titan*. Cambridge University Press, New York.  
347 doi:10.1017/CB09780511573071.

348 Horikawa, K., Hotta, S., Kubota, S., Katori, S., 1983. On the sand transport rate by wind on a beach. *Coast. Eng. Japan* 26, 101–120.

349 Horová, I., Koláček, J., Zelinka, J., 2012. Kernel Smoothing in Matlab: Theory and Practice of Kernel Smoothing.

350 ISO14688-1:2002. . Geotechnical investigation and testing - identification and classification of soil - part 1: Identification and description.

351 Iversen, J.D., Pollack, J.B., Greeley, R., White, B.R., 1976. Saltation threshold on mars: The effect of interparticle force, surface roughness, and  
352 low atmospheric density. *Icarus* 29, 381–93. doi:10.1016/0019-1035(76)90140-8.

353 Iversen, J.D., White, B.R., 1982. Saltation threshold on earth, mars and venus. *Sedimentology* 29, 111–9. doi:10.1111/j.1365-3091.1982.  
354 *tb01713.x*.

355 Jones, R., Pollock, H., Cleaver, J., Hodges, C., 2002. Adhesion forces between glass and silicon surfaces in air studied by afm: effects of relative  
356 humidity, particle size, roughness and surface treatment. *Langmuir* 18, 8045–8055. doi:10.1021/la0259196.

357 Kadib, A.L., 1964. Sand Transport by Wind - Addendum II to Sand movement by Wind. Technical Report 1. U.S. Army - Corps of Engineers. US  
358 Army Coastal Eng. Res. Center, Washington, DC.

359 Kawamura, R., 1951. Study of sand movement by wind. Technical Report. Translated (1965) as University of California Hydraulics Engineering  
360 Laboratory Report HEL 2-8. Berkley.

361 Kok, J.F., Parteli, E.J.R., Michaels, T.I., Karam, D.B., 2012. The physics of wind-blown sand and dust. *Rep. Prog. Phys.* doi:10.1088/  
362 *0034-4885/75/10/106901*.

363 Koláček, J., Zelinka, J., 2012. MATLAB toolbox. URL: [http://www.math.muni.cz/english/science-and-research/  
364 developed-software/232-matlab-toolbox.html](http://www.math.muni.cz/english/science-and-research/developed-software/232-matlab-toolbox.html).

365 Logie, M., 1981. Wind tunnel experiments on dune sands. *Earth Surf. Proc. Land.* 6, 365–374.

366 Logie, M., 1982. Influence of roughness elements and soil moisture on the resistance of sand to wind erosion. *Catena Suppl.* 1, 161–174.

367 Lyles, L., Krauss, R., 1971. Threshold velocities and initial particle motion as influenced by air turbulence. *Trans. ASAE* , 14563–14566.

368 McKenna, N.C., 2003. Effects of temperature and humidity upon the entrainment of sedimentary particles by wind. *Boundary Layer Meteorol.*  
369 108, 61–89. doi:10.1023/A:1023035201953.

370 McKenna Neuman, C., 2004. Effects of temperature and humidity upon the transport of sedimentary particles by wind. *Sedimentology* 51, 1–17.

371 McKenna Neuman, C., Nickling, W., 1989. A theoretical and wind tunnel investigation of the effect of capillary water on the entrainment of  
372 sediment by wind. *Can. J. Soil Sci.* 69, 79–96.

373 Merrison, J., 2012. Sand transport, erosion and granular electrification. *Aeolian Res.* 4, 1–16. doi:10.1016/j.aeolia.2011.12.003.

374 Middleton, N., Sternberg, T., 2013. Climate hazards in drylands: A review. *Earth-Sci. Rev.* 126, 48–57. doi:10.1016/j.earscirev.2013.07.  
375 *008*.

376 Nalpanis, P., Hunt, J.C.R., Barret, C.F., 1993. Saltating particles over flat beds. *J. Fluid Mech.* 251, 661–685. doi:10.1017/S00221120930035568.

377 Nicking, W.G., McKenna Neuman, N.C., 1997. Wind tunnel evaluation of a wedge-shaped aeolian sediment trap. *Geomorphology* 18, 333–345.  
378 doi:doi:10.1016/S0169-555X(96)00040-2.

379 Phillips, M., 1980. A force balance model for particle entrainment into a fluid stream. *J. Phys. D Appl. Phys.* 13, 221–233. doi:10.1088/  
380 *0022-3727/13/2/019*.

381 Pye, K., Tsoar, H., 2009. *Aeolian sand and sand dunes*. Springer. doi:10.1007/978-3-540-85910-9.

382 Rizvi, A., 1989. Planning responses to aeolian hazards in arid regions. *Journal of King Saud University, Architecture & Planning* 1, 59–74.

383 Roney, J.A., White, B.R., 2004. Definition and measurement of dust aeolian thresholds. *J. Geophys. Res.* 109. doi:10.1029/2003JF000061.

384 Saffman, P., 1965. Lift on a small sphere in a slow shear flow. *J. Fluid Mech.* 22, 385. doi:10.1017/S0022112065000824.

385 Shao, Y., 2008. *Physics and modelling of wind erosion*. 2nd ed., Springer. doi:10.1007/978-1-4020-8895-7.

386 Shao, Y., Lu, H., 2000. A simple expression for wind erosion threshold friction velocity. *J. Geophys. Res.* 105, 22437–43. doi:10.1029/  
387 *2000JD900304*.

388 Sheather, S.J., 2004. Density estimation. *Statistical Science* 4, 588–597. doi:10.1214/088342304000000297.

389 Sherman, D., Li, B., 2012. Predicting aeolian sand transport rates: A reevaluation of models. *Aeolian Res.* 3, 371–378. doi:10.1016/j.aeolia.  
390 *2011.06.002*.

391 Webb, N., Strong, C., 2011. Soil erodibility dynamics and its representation for wind erosion and dust emission models. *Aeolian Res.* 3, 165–179.  
392 doi:10.1016/j.aeolia.2011.03.002.

393 Zhang, C., Zou, X., Cheng, H., Yang, S., Pan, X., Liu, Y., Dong, G., 2007. Engineering measures to control windblown sand in shiquanhe town,

394 tibet. *J. Wind Eng. Ind. Aerod.* 95, 53–70. doi:[10.1016/j.jweia.2006.05.006](https://doi.org/10.1016/j.jweia.2006.05.006).  
395 Zhang, K., Chanpura, R.A., Mondal, S., Wu, C., Sharma, M.M., Ayoub, J.A., Parlar, M., 2014. Particle size distribution measurement techniques  
396 and their relevance or irrelevance to sand control design, in: *Proceedings of the 2014 SPE International Symposium and Exhibition on Formation*  
397 *Damage Control*, Lafayette, Louisiana, USA, February 26-28, 2014, Society of Petroleum Engineers.  
398 Zimon, A.D., 1982. *Adhesion of Dust and Powder*. Springer. doi:[10.1007/978-1-4615-8576-3](https://doi.org/10.1007/978-1-4615-8576-3).  
399 Zingg, A.W., 1953. Wind tunnel studies of the movement of sedimentary material, in: *Proceedings of the Fifth Hydraulic Conference*. *Studies in*  
400 *Engineering*, Iowa City, University of Iowa. pp. 111–35.